

Sedimentological and Geochemical Appraisal of Stream Sediments of Part of Igangan Sheet 240 South Western Nigeria

Owonipa Omoniyi Dare¹ Edema Abayomi^{2*}

1. Earth Sciences Department, Kogi State University, Anyigba, Nigeria
2. Geological Sciences Department, Achievers University, Owo, Nigeria

Abstract

An integrated sedimentological and geochemical evaluation was carried out on the sediments sampled from part of Igangan sheet 240 (1:100,000) SW Nigeria, covering Lanlate and its environs. This study is to characterize the provenance and depositional processes prevalent in the area. Twenty-nine stream sediment samples were collected after the confluence points of two or more rivers at a depth of 20-25cm, along with rock samples for further analyses in the laboratory. The techniques involved using standard sedimentological methods involving field descriptions, textural parameters, and petrographic analysis methods. The geochemical studies involved the determination of major elemental composition using Heavy Mineral analyses. Granulometric analysis was carried out on twenty-nine (29) stream sediments samples, while five (5) representative samples were systematically picked and analyzed for their mineralogical maturity using ZTR index. The rock samples were cut into thin section and analysed under the microscope for mineral composition. The results of the geochemical analysis were thereafter subjected to multivariate statistical analysis. The statistical plot shows that the sands are poorly sorted, medium to coarse grained and sub rounded to sub angular in shape. The sands which are medium to coarse grained suggests that the sands were deposited under a moderately energy condition. The field investigations and petrographic studies show that most of the study area has undergone an episode of metamorphism. Migmatite gneiss (80%), Biotite Hornblende Gneiss, quartzite (5%), muscovite hornblende biotite granite (10%) and biotite hornblende granite (5%) are the major rock in the area, while biotite, feldspar, quartz, hornblende and accessory minerals were observed in hand and thin sections. The calculated ZTR index for the sandstones ranges from 51.3% to 57.9 %, with an average of 54.6 %. This suggests that the sandstones of the formation are mineralogical mature. The conclusion drawn from the integration of the geochemical and multivariate analyses revealed that the study area is mineralized and the sediments were deposited under a moderate energy condition.

Keywords: *Igangan, Nigeria, Sedimentological, Stream sediments, Geochemical, Statistics*

1. Introduction

The textural parameters of surficial sands/sediments hold a lot of history regarding the provenance and environment of deposition of sediments in an area. This study was based on the geology and geochemical study of the sands and stream sediment samples collected from part of Igangan sheet 240 South-Western Nigeria; within the Nigeria basement Complex.

The area of study covers major villages like Lanlate, Maya, Lagaye, Ogodu, Duduyemi, Alaye, and environ. The area is geographically between Latitudes $3^{\circ}18'$ to $3^{\circ}30'$ and longitudes $7^{\circ}36'$ to $7^{\circ}42'$. It is an area covering about 288km^2 , a distance of about 12km by 24km. It is surrounded by basement rocks. The basement geology is characterized by distinct lithologies and mineralization. The sediment load of the river is predominantly those derived from the weathering of the surrounding basement rocks.

Geological Investigation in this part of Nigeria started in 1905, when the then mineral survey of Western Nigeria conducted reconnaissance survey in the region. Since then several other workers have contributed their own quota to the advancement of knowledge on these area. One of the earliest studies of the Nigerian basement complex was made by Fulconer (1911), when he distinguished the older granite from the younger granite. Oyawoye (1964) carried out a reconnaissance survey of the basement complex and gave a descriptive account of its geology. Jones and Hockey (1964) studied the south western basement complex. Rahman (1976) gives an explicit description of the petrology and geology of the basement complex. Burke et al (1972) worked on the structure and sequence of geological events in basement complex of Ibadan area. Emofurieta W.O. (1985) also worked on the geochemistry and petrography of two prominent Gneiss in the basement complex around South west Nigeria. Despite the research into the geology of the region, no reported work has addressed detailed studies on the sedimentology and paleoenvironment. In order to present detailed insight in understanding the

sedimentological events, a systematic mapping coupled with an extensive sampling and analyses was undertaken. This report incorporates the use of grain size analysis and heavy mineral analysis to determine the provenance (source) and the maturity index and to categorize the mechanism and environment of deposition using statistical parameters derived from the analysis.

2. Regional Geology of the Area

The Nigerian Precambrian Basement Complex bears the imprints of the Major orogenies in the earth history dating back to 3000 Ma and it undergone it most pervasive and remobilization during the Pan African (<600Ma) (Odeyemi, 1976). It lies in the extensive region, east of the West African Craton and Northwest of the Congo Craton. Evidences from the Eastern and Northern margins of the West African craton indicates that the Pan African belt evolved by tectonics processes which involved the collision between the passive continental margin of the West African Craton and the active continental margin of the Taureg shield about 600 Ma ago (Burkie and Dewey, 1972; Leblanc, 1981; Black *et al*; 1979; Cabyet *al*; 1987). Evidence for the collision includes the presence of basic to ultrabasic rocks believed to be either remnants of mantle diapirs or a paleo-oceanic crust, which has characteristics of an ophiolitic complex and a high positive gravity anomaly (Schluter, 2005). The collision of the plate margin is believed to have led to the reaction of the internal region of the belt. These Ancient Precambrian basement rocks were deformed during this period of earth movement known as the Pan African Orogeny (550 million years ago). They occupy about half the land area of Nigeria (Fig. 1). The basement rocks include mostly metasediments (gneisses, schists, migmatites and calc-silicates) along with amphibolites and rare metamorphosed tuffs and volcanic rocks. Banded iron formations, rich in magnetite and haematite, also exist in the basement.

3. Materials and Methods

A systematic mapping of the area was carried out, using a base map scale of 1:100,000. A good spread throughout the study area was ensured in the cause of the sampling and analysis. Representative rock samples were collected for petrographic studies. A total of 12 thin sections were prepared and examined with the aid of petrological microscope. The individual percentages of the minerals observed in the samples were computed based on point counting techniques.

A total of 29 stream sediment samples were collected after the confluence points of two or more rivers at a depth of 20-25cm, for geochemical analysis. These samples were subjected to grain-size analysis. The sediments were air-dried, disaggregated and sieved using the conventional sieving technique. The various statistical measures were interpreted based on Wentworth (1922), and Folk and Ward (1957), while Friedman (1967) bivariate plots were used for the determination of depositional environment.

5 selected sediment samples were further subjected to heavy mineral analysis. The term 'heavy mineral' generally applies to minor accessory mineral constituents of rocks having ordinarily specific gravities higher than 2.89g/cm^3 , which is the SG of bromoform (the preferable chemical). The heavy mineral concentrates was then mounted on slides using DPS mountant. The prepared slides was left on a hot plate for fifteen seconds and then viewed under the microscope for mineral identification and counting using the ribbon technique of Galehouse, (1971). This technique is useful in provenance studies and maturity determinations in sands and sandstones.

4. Results and Discussion

4.1 Field Occurrence and Characters

The rocks present in the study area are Migmatite Gneiss, Banded Gneiss, quartzite, porphyritic granite and fine grained granite (Fig. 2).

The migmatite is the oldest outcrop in the studied area. They occur as extensive low lying outcrops and as ridge-like hills, majority of them weathered. They are characterized by veins, veinlets and mineralized pegmatites. The light bands consist mainly of quartz and feldspars while the dark bands are enriched in mica (biotite). The intrusion and folding are indication of tectonic activities. Solution cavities are present on the migmatite which are the oldest rock present in the studied area.

The biotite hornblende gneiss occurs in the north eastern part of the map. The mesocratic medium grained gneiss characterized by conspicuous alternations of light and dark coloured bands is younger than the migmatite. They occurred as extensive low lying outcrops and are also highly weathered. They have not experience much tectonic

activities as found in migmatite, in terms of folding and weathering.

The quartzite occurs as a ridge trending in the NW-SE, and they exist as boulders at the SE part of the study area and thought to be derived from the metamorphism of deep seated intrusions. The quartzite boulders were not conspicuously exposed and majority of the exposed quartzite are weathered. They were highly jointed; a cross cutting joint.

The Muscovite hornblende biotite granite occurs as massive ridges occupying areas around Lanlate, SW part of the study area. They are generally leucocratic. They contain euhedral crystals of K-feldspars as phenocrysts with muscovite, quartz, biotite, plagioclase and hornblende in the coarse-grained groundmass. They have also been affected by various activities like biological weathering, exfoliation, shearing, brittle structures, depressions (solution holes) and intrusions. In some location, relics of the older rock unit were found (Xenolith) in the granite rock matrix. This signifies that this granite majorly intrudes the older rock. They occupied more than 30% of the studied area.

The biotite hornblende granite occurs as massive ridges. They have also been affected by various activities as found in the porphyritic granite. They are fine to medium grained. They are the youngest of the rock occurring in the studied area. They are also major plutonic rock that intruded the older rock unit. Xenoliths of the older rock unit were also found in the rock matrix. They occupied up to 10% of the studied area.

Some minor rock units have also intruded the entire rock unit in the form of veins and veinlet. They occupied the line of weakness of the Major rock unit, i.e. the joint, fracture, fault planes etc. They are younger than the rock units they intruded. The veins and veinlets contain large percentage of quartz and feldspar (Quartzofeldspatic) while the pegmatites are highly mineralized. The main minerals of pegmatite are quartz and feldspar. They are coarsely grained. The dolerite occurs as a dyke. The dyke has joint which cut across it and trending 132. The dyke measured 40cm thick and 1960cm wide.

Structural features like joints, fold, lineations, foliations, exfoliations, boudinage, fracture, faults, solution cavities, xenoliths, bands and veins were seen on the field. The trends of the structures were measured and rosette diagrams were plotted for each to determine their directions (Fig.4). The joint are trending in the NE-SW while the veins, foliations, fold, and the lineation are trending in the NW - SE direction.

4.2 Petrographic Characteristics

The modal compositions of the minerals observed from thin section (Fig. 5) studies of the rock samples collected from the study area, are presented in Table 1.

The Quartz Crystals have rounded edges and overgrowths of quartz at the edges of the original crystals. There are intergrowth of quartz and feldspar (mymerkite) in some slides. It also occurs as the groundmass. Some of the crystals show undulose extinction; this suggests that the crystals have been subjected to strain. These crystals are colourless in PPL with low relief. It is the most abundant mineral in the rocks.

The Plagioclase crystals are colourless in PPL, with a low relief and oblique extinction. Crystals show repeated albite twinning.

The Microcline crystals are pale green in colour and pleichroic with perfect cleavage in one direction with parallel extinction. They occur as thin tabular crystals, scaly aggregates with intergrowth of felspar and quartz.

The Biotite crystals have a light to dark brown colour in thin section. It's a platy crystal with one cleavage direction.

The Hornblende crystals in thin-section are observed to alternate from a distinct green to a brown colour when rotated and have moderate relief in ppl.

The Garnet crystals are colourless in PPL with brown inclusions. They have well formed crystals dark brown in XPL with no cleavage.

4.3 Textural Characteristics

The individual fraction retained in each sieve was carefully weighed with the sieve. The retained Sample weight(S) = Weight of Sieve and sample (SW) - Sieve weight (W) (Table 2). The percentage of each fraction of the weight retained was calculated for each soil sample i.e. (weight retained/ actual total weight) * 100. The cumulative weight percentage was derived from the percentage weight. Cumulative curves (Ogive curve) were plotted using the cumulative weight percentage (y axis) against the equivalent phi values(x axis) (Fig.5A). The values Φ_5 , Φ_{16} , Φ_{25} , Φ_{50} , Φ_{75} , Φ_{84} , Φ_{95} were obtained from the Ogive curve. These values were then used to calculate the textural parameters (Table2, 3 and 4), which were used for further interpretation of our analysis

results. The parameters were interpreted based on Univariate and Bivariate analysis. The Univariate Interpretation was based on only one parameter respectively (Table 5). The mean size indicates a measure of central tendency or in this scenario the average size of the sediment. Translated in terms of energy, it indicates the average kinetic energy (velocity) of the depositing agent (Sahu 1964). The mean grain size of the sediment samples range from 0.01 to 1.27 Φ , indicating coarse to medium sands. The standard deviation measures the sorting of the sediments and indicates the fluctuation of the kinetic energy (velocity) conditions of the depositing agent about its average velocity. Sorting deduced for the samples ranges from 1.02 to 1.52 which implies that the sands are commonly poorly sorted. Skewness measures the degree of asymmetry of the frequency distribution and marks the position of the mean with respect to the median. Skewness values are negative ranging from -0.11 to 0.54 which implies that the sands are from nearly symmetrical to Very positively skew. Kurtosis values ranges from 0.65 to 2.10 which imply very kurtic to very leptokurtic. Kurtosis is conventionally considered as a measure of the peakedness of the frequency curve, however, Kendall and Stuart (1958) believes that it is not necessarily so and that the kurtosis should not be interpreted as describing the shape of the frequency curve. By definition, kurtosis measures the sorting ratio and not the peakedness of the frequency curve. For normal distributions, kurtosis is unity, values greater than unity indicates that the velocity fluctuations were restricted within the central 50% of the average velocity for a greater length of the time than normal. On the average the samples are describes as platykurtic.

When two statistical parameters are combined to interpret the depositional environment, we describe the analysis as bivariate analysis. This has successfully been used by Friedman (1961) and Visser (1969). The plot of the sorting against mean sizes (Fig.6) shows the point all clustering in a particular area except samples 2 and 9. This shows that the same mechanism of deposition was common to all the samples for them to plot in like fields. Cross plot of skewness against sorting (Friedman 1967) (Fig.8) shows that the sediments fall within river sand.

Notice that all the plots fell on the river sands field of the plot, this goes to confirm the Univariate analysis that the sediment are from a fluvial environment. From the field relationship, within the Basement Complex the only medium of transportation of the sediments weathered from the rocks is the river and surface run-offs predominantly, less of wind and dune mechanism maybe nil.

From the analysis above the sediments from the area is best described as being very fine to medium grained, poorly sorted, near symmetrical mesokurtic sands. This description is common to river sands whose energy is typical to that of the fluvial depositional environment.

4.4 Geochemical Characteristics

The photomicrograph of the thin section of sample 4, 9, 10, 15, 22 and 25 are presented in Fig 9 above. The minerals counts identified are presented on table 6. The significance of heavy minerals to solving geologic problems associated with provenance and stratigraphic horizon discrepancies cannot be over-emphasized. A total of about 1127 heavy minerals were counted in the study area with a total of 537 non-opaque minerals whose properties we studied. The dominant mineral in the area studied was zircon which was followed by Tourmaline and then Rutile These three minerals incidentally are regarded as the ultrastable heavy minerals and hence because of this Hubberd (1975) successfully used them to determine the maturity of sandstones based on their indices. The ZTR index of the study area was calculated and seen to range from 54.2% to 62.8% among the samples analysed. The ZTR index was determined using the relationship given below:

$$ZTR\ index = \frac{Z + T + R}{Non - Opaque}$$

A ternary diagram having zircon –tourmaline – rutile as apices was plotted and it had all the samples plotting in the same field indicating the same environmental conditions affecting them, and that there are from the same source (Fig. 10).

The maturity of sandstones can be determined with the combined studies of quartz crystals which was not analyzes in our study, however, from the values obtained, it shows that the samples although they have not travelled far from their source, they are at the verge of attaining maturity. Kyanite and glaucophane were present in the counts in small quantity, but their presence combined with the predominance of zircon (a rock that occurs in both igneous and metamorphic terrain) and tourmaline, points to the rocks of the Basement Complex as the source of these clastics and judging from the well formed crystals and sub-angular crystals observed, it can be said that the grains have not travelled too far from their source (i.e. the provenance can be traced to the vicinity

of the rocks of the basement complex). Feo-codecido (1955) presented a table that characterizes the heavy mineral suite one may likely find in certain environments (Table 7).

5. Conclusion

A functional structure made up of holons is called holarchy. The holons, in coordination with the local environment, function as autonomous wholes in supra-ordination to their parts, while as dependent parts in subordination to their higher level controllers. When setting up the WOZIP, holonic attributes such as autonomy and cooperation must have been integrated into its relevant components. The computational scheme for WOZIP is novel as it makes use of several manufacturing parameters: utilisation, disturbance, and idleness. These variables were at first separately forecasted by means of exponential smoothing, and then conjointly formulated with two constant parameters, namely the number of machines and their maximum utilisation. As validated through mock-up data analysis, the practicability of WOZIP is encouraging and promising.

Suggested future works include developing a software package to facilitate the WOZIP data input and conversion processes, exploring the use of WOZIP in the other forms of labour-intensive manufacturing (e.g. flow-line production and work-cell assembly), and attaching a costing framework to determine the specific cost of each resource or to help minimise the aggregate cost of production.

References

- Black, R.H., Ba, E., Ball, J.M.L., Bertrand A.M., Boullier, R., Carby, I., Davingson, J., Fabre, M. Leblanc and Wright, L.I (1979). Outline Of The Panafrican Geology Of Adrar Dex Iforas (Rep. Of Mali). *Geol.Rundsch*, 69(2) 543-564.
- Burke, K. C., and Dewey, F. J. (1972). Orogeny in Africa. In *African Geology* Ibadan, 1970. Eds.Dessauvague and Whiteman. Geol. Dept. Univ. Ibadan, Nigeria. P.583.
- Caby, R., Bertrand, J.M.L., and Black R., (1981). Pan-African Ocean closure and continental collision in the Hogger – Iforas segment. *Central Saharai in Precambrian plate Tectonics* edited by A. Kroner, Elsevier Amsterdam pp. 407 – 434.
- Elueze, A.A. (1992). RIFT System Of Proterozoic Scist Belts In Nigeria, *Tectonophysics*, 209, Pp. 167-169.
- Feo-Codecido G. (1955). Heavy Mineral Techniques and their Application to Venezuelan Stratigraphy. *AAPG Bull.* Vol 40/5, pp 984 – 1000.
- Folk, R.L., Ward, W.L.1957. Brazus River Bar: A Study of the Significance of Grain Size Parameters. *J. Sed. Petrology.* Vol 27, pp 3-27.
- Friedmann, G.M.J. (1961). Distribution Between Dune, Beach And River Sands From Their Textural Characteristics *J.Sed. Petrology*, pp 31, 514-529.
- Friedmann, G.M., (1967). Dynamic Processes And Statistical Parameters Compared For Size Frequency Distribution Of Beach And River Sands. *J.Sed. Petrology*, 37, pp 327-354.
- Falconer, J.D. (1911). *The Geology and geography of Nigeria* MacMillian, London.
- Galehouse, J. S. (1971). Counting grain mounts: Number percentage vs number frequency. *Notes: J.Sed. Petrology*, 22, pp 125 – 145.
- Hubbard, F.H., (1975). Precambrian Crustal Development In Western Nigeria: Indications From The Iwo Region. *Bull. Geol. Soc Am.*, 86: 548-554.
- Jones, H.A. , Hockey, R.D. (1964). The geology of part of Southwestern Nigeria. *Nigeria Geol. Surv. Bull.* No.31 87pp.
- Kendall, M.C., ., Stuart, A., (1958). *The Advanced Theory of Statistics.* Vol.1 Griffin And Co.Ltd. London.
- Leblanc, M. (1981). The Late Proterozoic Ophiolites Of Bou Hazzar (Morocco) Evidence For Pan African Plate Tectonic In *Precambrian Plate Tectonics*, Edited By A.Kroner, Elsevier, Amsterdam: Pp 435-451.
- Odeyemi, I.B., (1976). Preliminary report on the field Relationships of Basement Complex Rocks and Igara, mid western Nigeria. In: Kogbe, C A (Ed) *Geology of Nigeria*, Elizabethan Publishing Company Lagos, pp

58-63.

Oyawoye, M.O. (1964). The Geology of the Nigerian Basement Complex. Journ. Nigerian Min. geol. And Metall. Soc. Vol. 1.

Rahaman, M. A. (1976). Review of the basement geology of the southwestern Nigeria. In Kogbe, C. A. (ed), Geology of Nigeria. Elizabeth Publishing Co., Surulere, Lagos, pp 41- 58.

Sahu, B. K. (1964). Depositional Mechanism from the Size Analysis of Clastic Sediments. Jour. Sed. Petrology. Vol 34/1.pp 73 – 83.

Schluter, T. (2005). Geological Atlas of Africa: with Notes on Stratigraphy, tectonics, economic geology, geohards, geosites and geoscientific education of each contry 2nd edition. Springer, 272p.

Visher, G. S. (1969). Grain size distribution and depositional processes. J. Sed. Petrology, 34, pp 1074 – 1106.

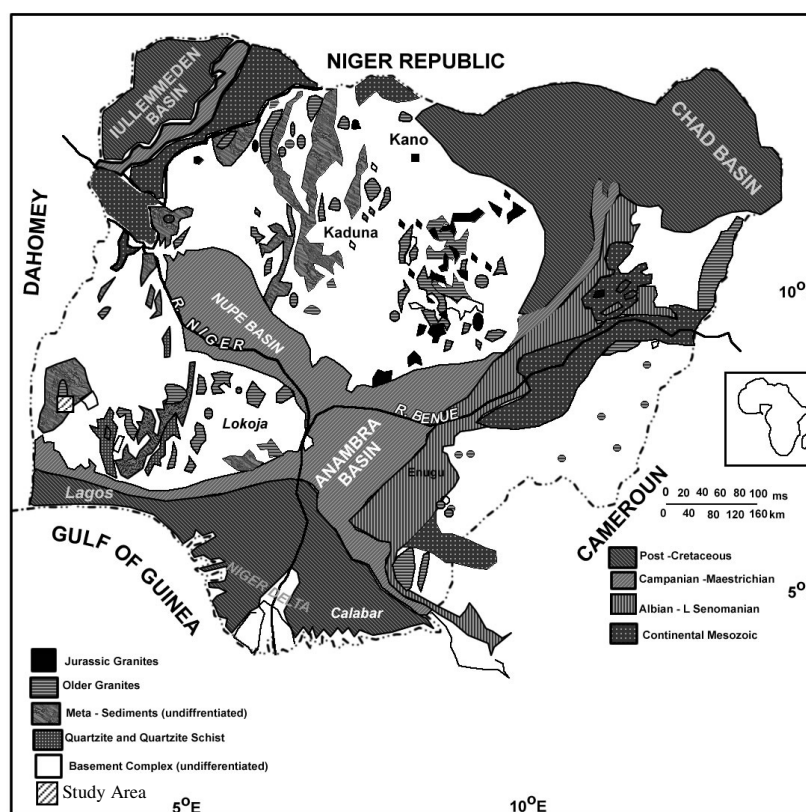


Figure 1. Compilation Map Of The Geology Of Nigeria (Geological Survey Of Nigeria) Showing Study Area Adapted After Elueze, 1992.

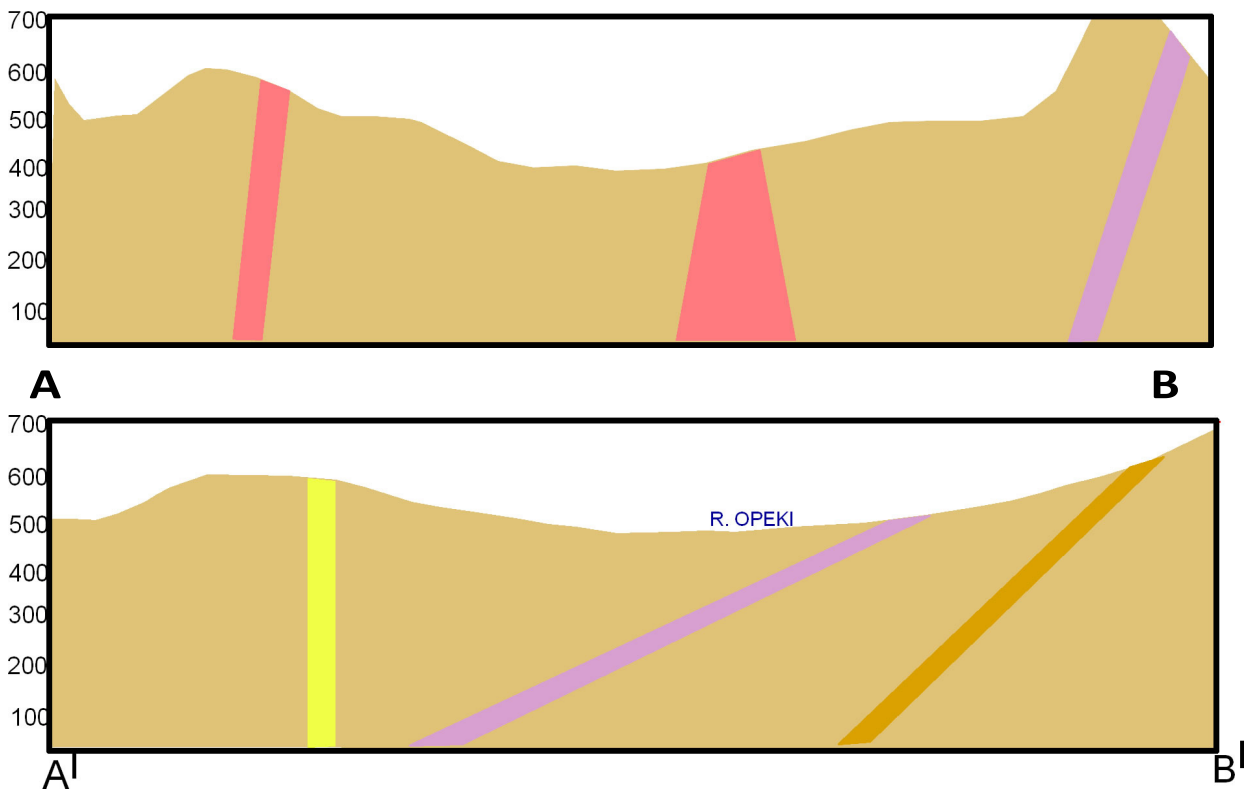
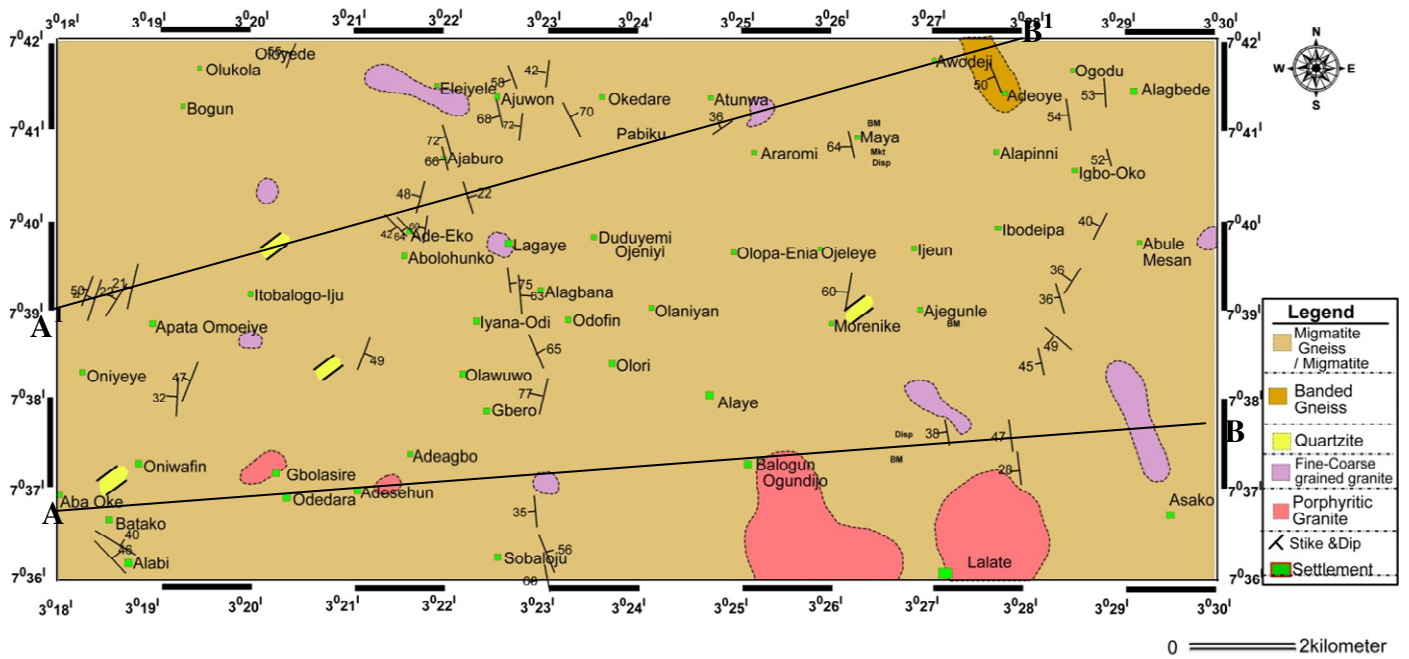


Figure 2. A Geological Map of Lanlate And Its Environs, A Part of Igangan Sheet 240 South-Western Nigeria 1:100 000

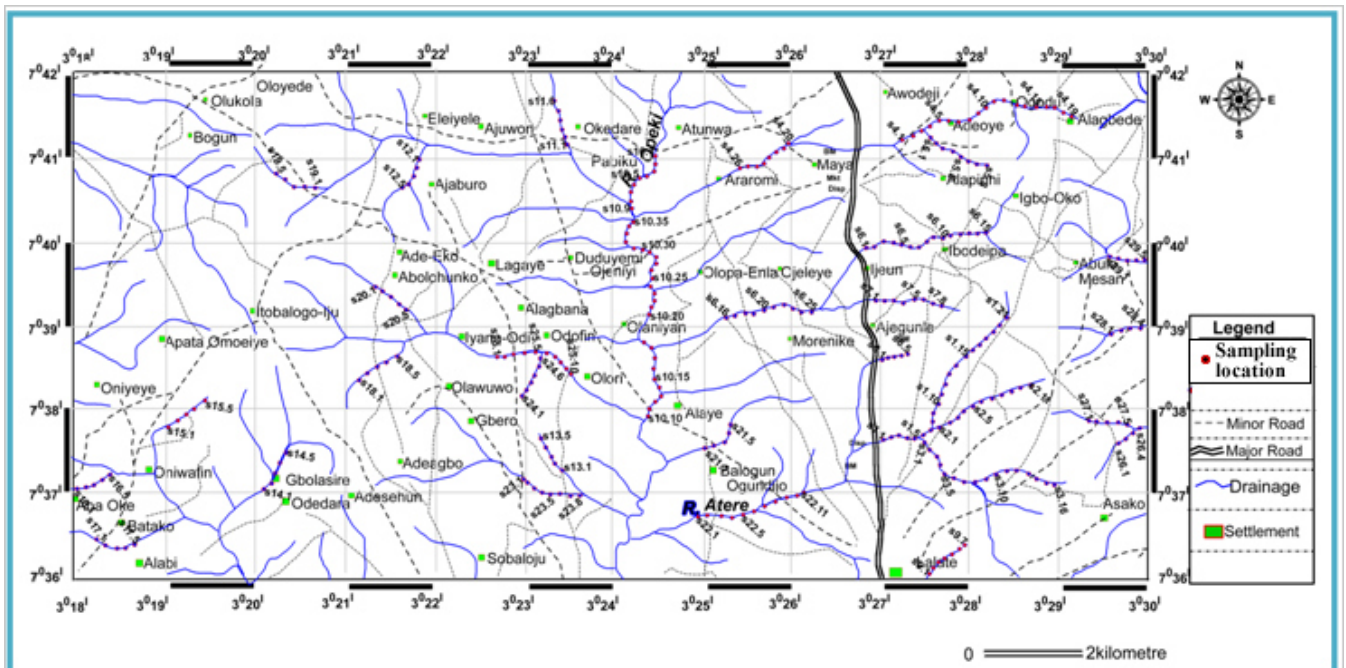


Figure 3. A Geological Map of Lanlate And Its Environs, A Part of Iangan Sheet 240 South-Western Nigeria 1:100 000

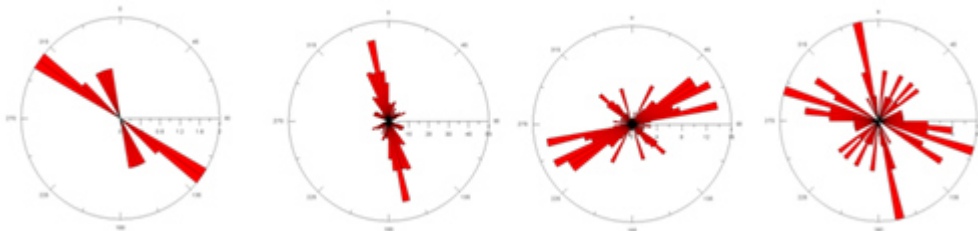


Figure 4. Rosette Diagrams Showing A. Trending Direction of the Lineation NW-SE, B. Foliation Trends, C. Orientation Of Joints, D. Orientation Of Veins

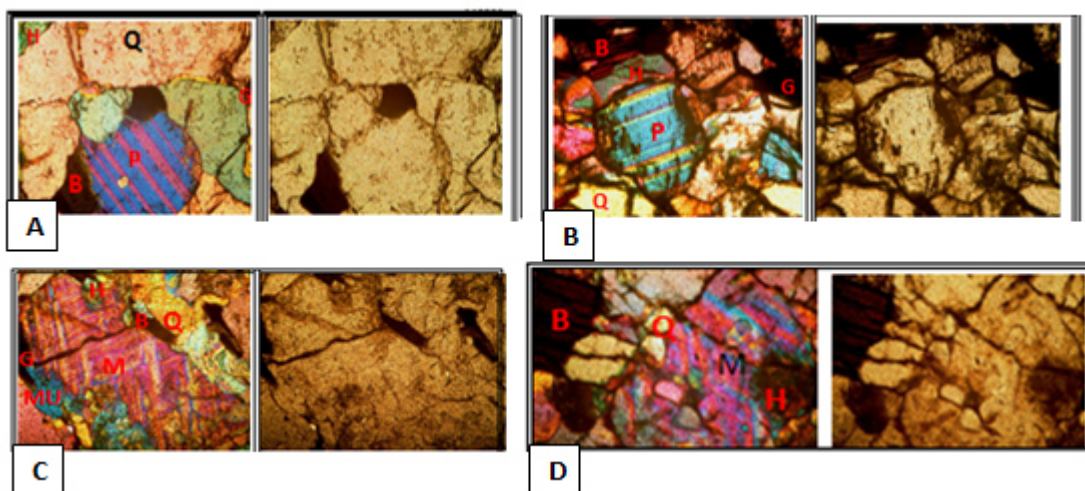


Fig. 5: Photomicrograph showing sample of rock present in the study area under cross and plain polarised light a. Migmatite Gneiss b. Banded Gneiss, c. Porphyritic Granite, d. fine grain Granite. Q=Quartz, B=Biotite, M=Microcline, H=Hornblende, G=Garnet, P=Plagioclase,

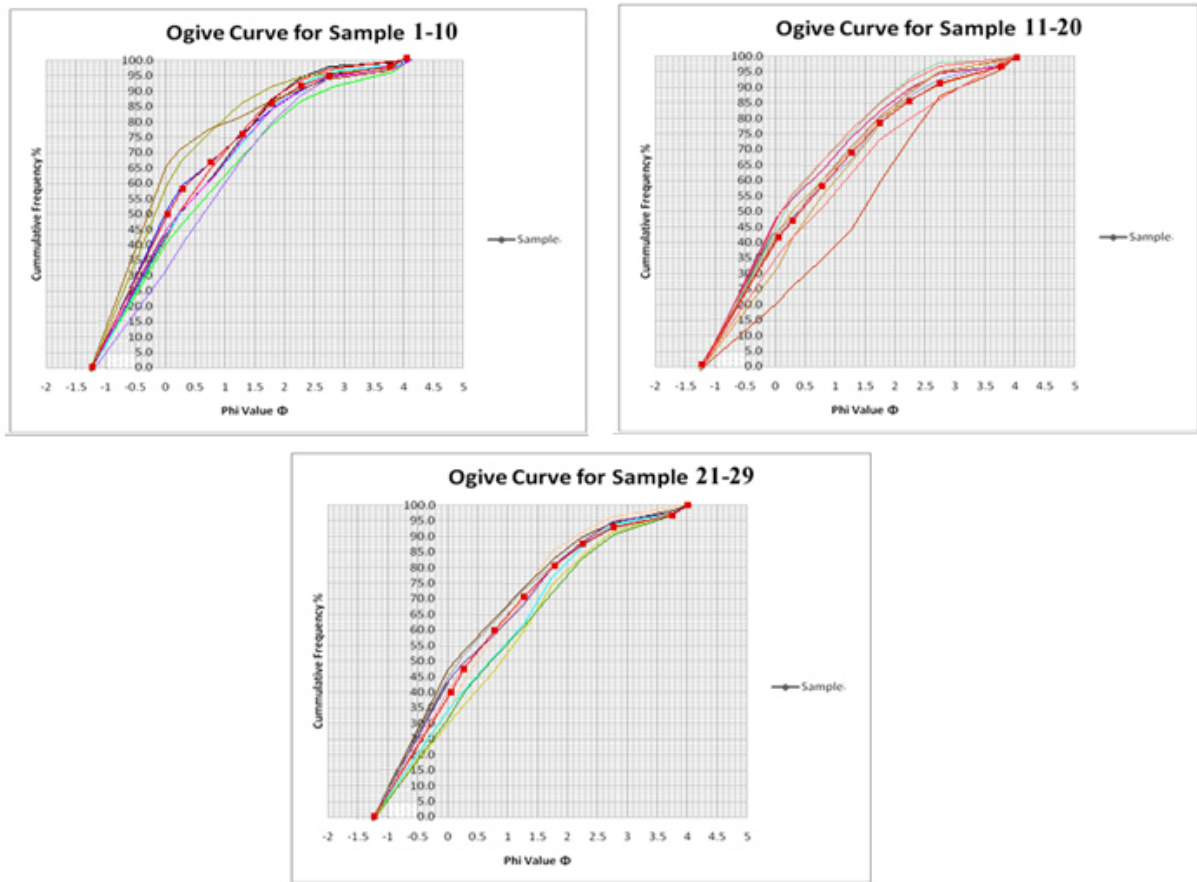


Figure 5. Cumulative Curves (Ogive Curve) Plotted Using The Cumulative Weight Percentage (Y Axis) Against The Equivalent Phi Values(X Axis)

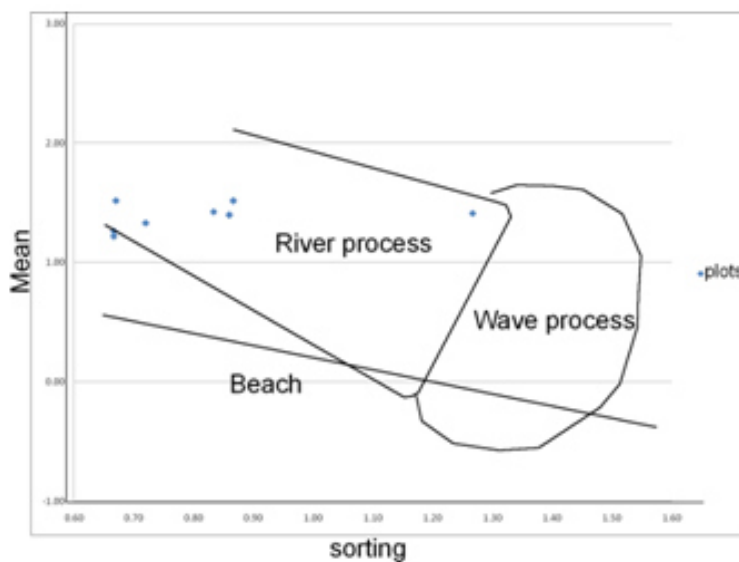


Figure 6: Bivariant plot of Sorting against Mean after Friedman (1961)
 This show the sediment of fluvial origin. i.e. continental depositional environment

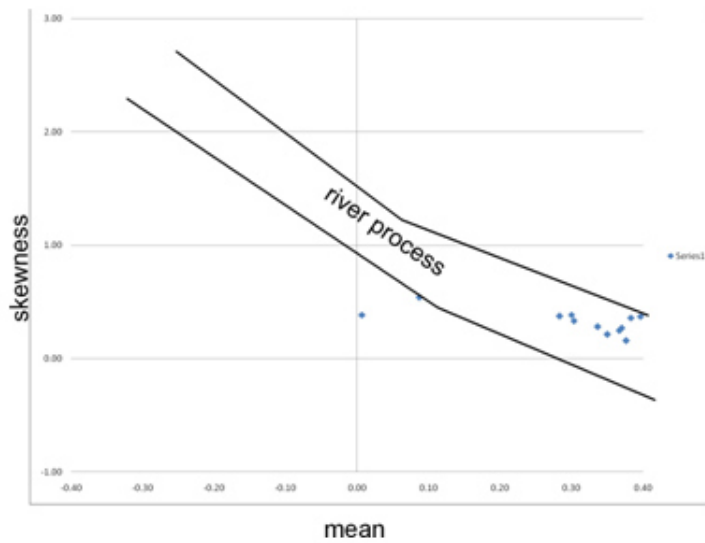


Figure 7: Bivariate plot of Mean against Skewness after Friedman (1961)
This show the sediment of fluvial origin

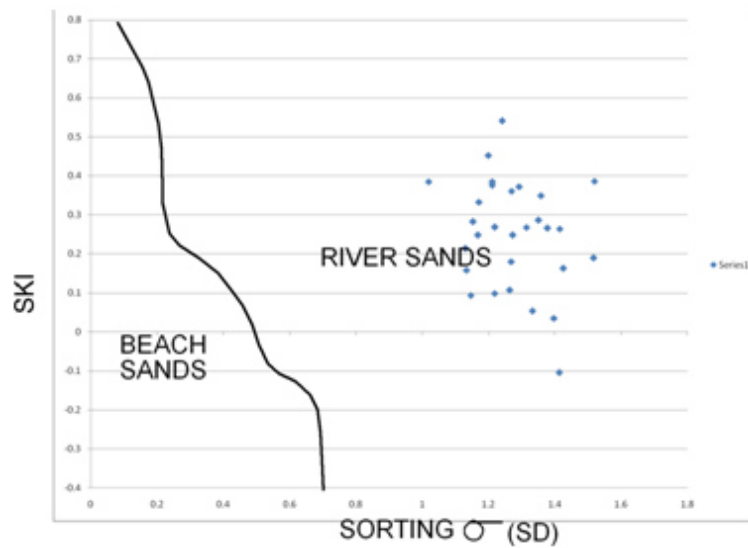


Figure 8: Bivariate plot of Sorting against Skewness after Friedman (1961)
This show the sediment has not experienced much transportation but have been moved some distance from their sources

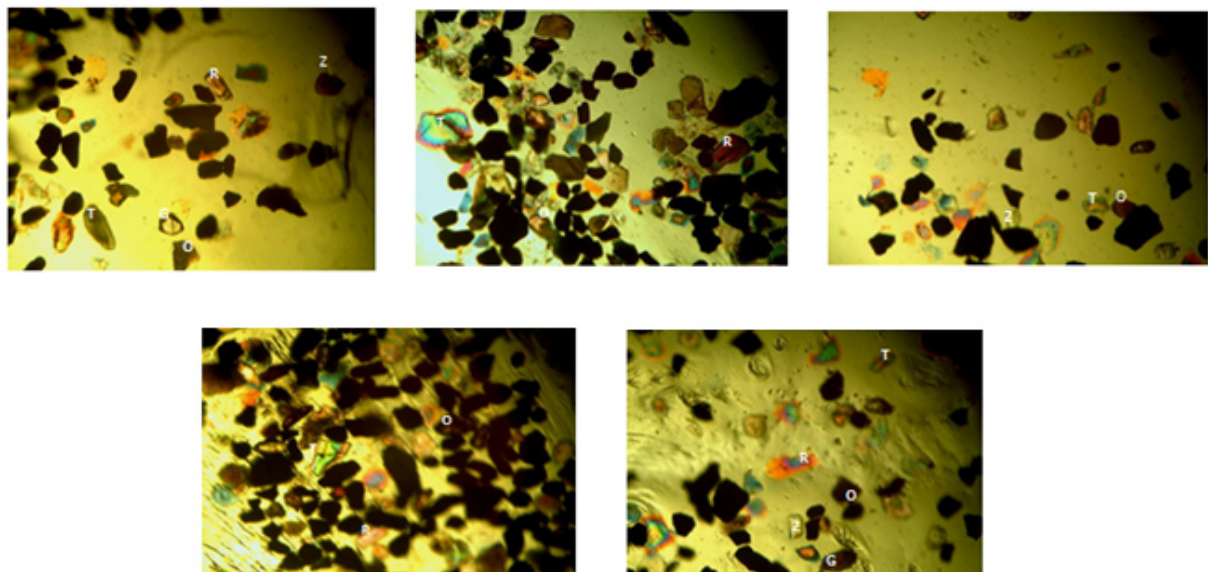


Figure 9: The Photomicrograph of Stream Sediments Sample 4, 9,10,15,22 and 25

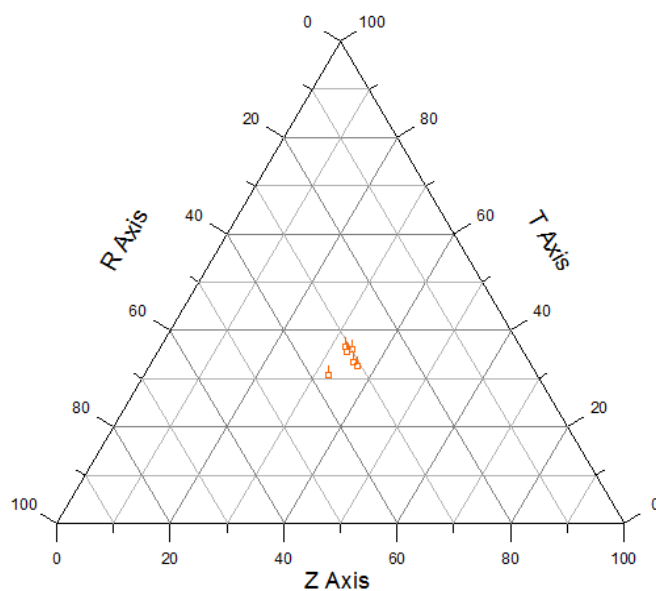


Figure 10: A ternary diagram of Zircon, Tourmaline and Rutile from the study area

Table 1. Modal Composition of Observed Minerals from the Thin Sections

MINERALS	MIGMATITE GNEISS	BANDED GNEISS	PORPHYRITIC GRANITE	BIOTITE HORNBLEND GRANITE
Quartz	50%	20%	25%	40%
Plagioclase	25%	30%	15%	-
Microcline	-	-	36%	35%
Biotite	10%	15%	15%	10%
Hornblend	5%	5%	5%	5%
Muscovite	-	-	-	5%
Garnet	3%	15%	-	-
Accessory		15%	4%	5%

Table 2: Weight Retained In the Respective Sieves

Samples	SIEVE SIZES									TOTAL
	1mm	850µm	600µm	425µm	300µm	212µm	150µm	75µm	<75µm	
1	65	10	18	19	18	11	5	3	1	150
2	62	15	20	17	16	10	6	3	1	150
3	61	10	16	17	14	12	8	7	5	150
4	77	12	12	14	12	9	7	4	3	150
5	65	13	15	17	17	11	7	3	3	150
6	68	9	17	16	17	9	6	4	4	150
7	74	12	13	14	14	9	6	4	4	150
8	98	9	9	6	8	5	6	4	5	150
9	89	12	15	13	8	5	2	2	4	150
10	48	12	21	21	17	14	8	7	2	150
11	64	8	14	15	18	13	7	7	4	150
12	68	13	17	15	15	12	6	2	2	150
13	72	9	14	15	13	11	7	4	5	150
14	30	7	14	15	24	21	20	12	7	150
15	62	9	18	17	16	10	10	6	2	150
16	64	11	14	15	16	9	8	8	5	150
17	47	13	21	19	19	14	10	5	2	150
18	62	9	16	15	15	11	9	8	5	150
19	53	8	16	17	16	11	8	17	4	150
20	72	12	15	15	14	10	7	4	1	150
21	62	12	14	15	18	11	10	5	3	150
22	53	13	22	21	19	10	6	4	2	150
23	60	129	18	16	15	10	8	6	5	150
24	52	9	15	17	22	15	10	6	4	150
25	45	9	16	18	23	15	11	8	5	150
26	48	12	16	15	18	15	12	9	5	150
27	70	9	16	15	14	10	7	6	3	150
28	66	8	13	15	17	13	9	5	4	150
29	68	9	16	16	12	10	8	6	5	150

Table 3: Phi (Φ) Values Obtained From the Cumulative Curves

Sample	5	16	25	50	75	84	95
1	-1.1	-0.8	-0.5	0.28	1.29	1.65	2.34
2	-1.1	-0.78	-0.5	0.21	1.22	1.62	2.4
3	-1.1	-0.75	-0.5	0.38	1.54	2.08	3.32
4	-1.1	-0.85	-0.62	0	1.15	1.7	2.68
5	-1.1	-0.79	-0.51	0.19	1.32	1.7	2.5
6	-1.1	-0.8	-0.55	0.2	1.31	1.71	2.8
7	-1.1	-0.81	-0.6	0.01	1.22	1.7	2.75
8	-1.12	-0.94	-0.76	-0.3	0.5	1.5	3.04
9	-1.11	-0.9	-0.71	-0.2	0.61	1.12	2.28
10	-1.15	-0.6	-0.25	0.6	1.54	2	2.9
11	-0.11	-0.79	-0.51	0.35	1.57	2	3.2
12	-1.1	-0.8	-0.55	0.12	1.25	1.69	2.4
13	-1.1	-0.8	-0.6	0.1	1.35	1.89	2.99
14	-0.9	-0.25	0.28	1.45	2.3	2.6	3.72
15	-1.1	-0.78	-0.5	0.4	1.44	1.93	2.8
16	-1.1	-0.8	-0.51	0.25	1.5	2.56	3.38
17	-1.05	-0.6	-0.22	0.6	1.59	2	2.7
18	-1.1	-0.78	-0.5	0.4	1.6	2.15	3.4
19	-1.08	-0.69	-0.38	0.7	1.85	2.59	3.52
20	-1.1	-0.82	-0.6	0.05	1.2	1.68	2.5
21	-1.09	-0.78	-0.5	0.3	1.5	1.96	2.79
22	-1.08	-0.69	-0.35	0.46	1.35	1.7	2.54
23	-1.1	-0.59	-0.48	0.32	1.47	1.99	3.29
24	-1.08	-0.6	-0.35	0.74	1.69	2.11	3.09
25	-1.1	-0.8	-0.2	0.9	1.8	2.27	3.4
26	-1.05	-0.6	-0.25	0.72	1.85	2.38	3.44
27	-1.1	-0.8	-0.6	0.1	1.35	1.85	2.9
28	-1.1	-0.8	-0.55	0.29	1.56	2	2.95
29	-1.1	-0.8	-0.55	0.19	1.4	2	3.24

Table 4: The Results for Statistical Parameters

Sample	Mean	Sorting/S.D	Skewness	Kurtosis
1	0.38	1.13	0.16	0.79
2	0.35	1.13	0.21	0.83
3	0.57	1.38	0.27	0.89
4	0.28	1.21	0.38	0.88
5	0.37	1.17	0.25	0.81
6	0.37	1.22	0.27	2.1
7	0.3	1.21	0.38	0.87
8	0.09	1.24	0.54	1.35
9	0.01	1.02	0.39	1.05
10	0.67	1.26	0.11	0.93
11	0.52	1.2	0.45	0.65
12	0.34	1.15	0.28	0.8
13	0.4	1.29	0.37	0.86
14	1.27	1.41	-0.11	0.94
15	0.52	1.27	0.18	0.82
16	0.67	1.52	0.39	0.91
17	0.67	1.22	0.1	0.85
18	0.59	1.41	0.26	0.88
19	0.87	1.52	0.19	0.85
20	0.3	1.17	0.33	0.82
21	0.49	1.27	0.25	0.8
22	0.49	1.15	0.09	0.87
23	0.52	1.35	0.29	0.92
24	0.72	1.33	0.05	0.84
25	0.86	1.4	0.03	0.92
26	0.83	1.43	0.16	0.88
27	0.38	1.27	0.36	0.84
28	0.5	1.31	0.27	0.79
29	0.46	1.36	0.35	0.91

	Mean	Sorting	Skew	Kurtosis
Min	0.01	1.02	-0.11	0.65
Max	1.27	1.52	0.54	2.1

Table 5: Summary for The Interpretation Of Univariate Analysis

Sample	Mean	Sorting	Skewness	Kurtosis
1	Coarse Sand	Poorly Sorted	Positively Skewed	Platykurtic
2	Coarse Sand	Poorly Sorted	Positively Skewed	Platykurtic
3	Coarse Sand	Poorly Sorted	Positively Skewed	Platykurtic
4	Coarse Sand	Poorly Sorted	Very Positively Skewed	Platykurtic
5	Coarse Sand	Poorly Sorted	Positively Skewed	Platykurtic
6	Coarse Sand	Poorly Sorted	Positively Skewed	Very Leptokurtic
7	Coarse Sand	Poorly Sorted	Very Positively Skewed	Platykurtic
8	Coarse Sand	Poorly Sorted	Very Positively Skewed	Leptokurtic
9	Coarse Sand	Poorly Sorted	Very Positively Skewed	Mesokurtic
10	Coarse Sand	Poorly Sorted	Positively Skewed	Mesokurtic
11	Coarse Sand	Poorly Sorted	Very Positively Skewed	Very Kurtic
12	Coarse Sand	Poorly Sorted	Positively Skewed	Platykurtic
13	Coarse Sand	Poorly Sorted	Very Positively Skewed	Platykurtic
14	Medium Sand	Poorly Sorted	Nearly Symmetrical	Mesokurtic
15	Coarse Sand	Poorly Sorted	Positively Skewed	Platykurtic
16	Coarse Sand	Poorly Sorted	Very Positively Skewed	Mesokurtic
17	Coarse Sand	Poorly Sorted	Positively Skewed	Platykurtic
18	Coarse Sand	Poorly Sorted	Positively Skewed	Platykurtic
19	Coarse Sand	Poorly Sorted	Positively Skewed	Platykurtic
20	Coarse Sand	Poorly Sorted	Very Positively Skewed	Platykurtic
21	Coarse Sand	Poorly Sorted	Positively Skewed	Platykurtic
22	Coarse Sand	Poorly Sorted	Positively Skewed	Platykurtic
23	Coarse Sand	Poorly Sorted	Positively Skewed	Mesokurtic
24	Coarse Sand	Poorly Sorted	Nearly Symmetrical	Platykurtic
25	Coarse Sand	Poorly Sorted	Nearly Symmetrical	Mesokurtic
26	Coarse Sand	Poorly Sorted	Positively Skewed	Platykurtic
27	Coarse Sand	Poorly Sorted	Very Positively Skewed	Platykurtic
28	Coarse Sand	Poorly Sorted	Positively Skewed	Platykurtic
29	Coarse Sand	Poorly Sorted	Very Positively Skewed	Mesokurtic

Table 6: The Counts Of Heavy Minerals Identified On The Photomicrograph

Sample No.	Z	T	R	H	B	G	Gl	St	A	Ky	Non- Opaque	Opaque Minerals	ZTR Index %
4	16	15	18	0	1	13	0	15	-	-	78	32	62.8
9	17	19	16	2	4	17	8	16	11	3	113	153	46
10	17	18	15	-		17	-	15	-	-	82	47	61
15	15	16	14	-	1	18	-	16	-	-	80	104	65.3
22	18	16	15	8		17	3	15	6	3	101	131	48.5
25	16	15	14	3		14	3	16	2	-	83	123	54.2
	99	99	92	13	6	96	14	93	19	6	537	590	

Z=Zircon,T=Tourmaline,R=Rutile,H=Hornblende,B=Biotite,G=Garnet,Gl=Glaucothane,
 St=Staurolite,A=Apatite,Ky=Kyanite,ZTR index in %.

Table 7: Heavy Mineral Associations and Provenance

Associations	Source
Apatite, Biotite, Brookite, Hornblend, Monzonite, Muscovite, Rutile, Titanite, Tourmaline, (Pink Variety), Zircon.	Acid Igneous Rocks
Cassiterite, Dumortierite, Fluorite, Garnet, Monazite, Muscovite, Topaz, Tourmaline (Blue Variety), Wolframite, Xenotime	Granite Pegmatites
Augite, Chromite, Diopside, Hypersthene, ilmenite, magnetite, olivine, Picotite, Pleonaste	Basic Igneous Rocks
Andalusite, Chondrodite, Corundum, Garnet, Phlogopite, Staurolite, Topaz, Vesuvianite, Wollastonite, Zoisite.	Contact Metamorphic Rocks
Andalusite, Chloritoid, Epidote, Garnet, Glaucothane, Kyanite, Sillimanite, Staurolite, Titanite, Zoisite-clinozoisite	Dynamothermal Metamorphic Rocks
Barites, Iron ores, Leucocoxene, Rutile, Tourmaline (Rounded Fragments), Zircon (Rounded Fragments)	Reworked Sediments